J of Nuclear Medicine Technology, first published online September 28, 2021 as doi:10.2967/jnmt.120.256917

Title Page:

**Predictive model for rubidium-82 generator bolus times as a function of generator lifetime**

Alexander W. Scott [1], Mark Hyun [1], Jennifer Kim [2]

[1] Department of Imaging, Cedars-Sinai Medical Center

[2] Department of Clinical Research Operations, City of Hope

Disclaimer:

Corresponding and first author

Alexander Scott,

8705 Gracie Allen Dr., Taper M335

Los Angeles, CA 90048

(310) 423-9536

Alexander.Scott@cshs.org

Word Count: 2661

COI disclosure statement:

Mark Hyun: “I served as a technical consultant to Astellas regarding the Lexiscan product. No other potential conflicts of interest relevant to this article exist.”

Alexander W. Scott, Jennifer Kim: "No potential conflicts of interest relevant to this article exist."

Running title “**Predictive model for an 82Rb generator”**

Rationale: 82Rb cardiac PET is largely used to study myocardial perfusion with function, and to calculate myocardial blood flow (MBF) and coronary flow reserve (CFR) or myocardial flow reserve (MFR). Although the dosing activity of 82Rb is determined by the patient weight, the infusion volume and activity concentration varies with the age of the 82Rb generator. We sought to predict the needed bolus volume of 82Rb to help evaluate the accuracy of MBF findings.

Methods: Data was collected from de-identified tickets of an 82Rb generator, including the instantaneous eluted activity flow rate. The times to reach 4 activity levels of 20, 30, 40, and 45 mCi (740, 1110, 1480, and 1665 MBq respectively) were also calculated. The activity flow rate for the largest bolus was fitted to determine the functional form. The time to reach each bolus level was fitted as a function of the generator age and 95% confidence limits were created.

Results: The activity flow rate was fitted with a growth-saturation model, allowing a calculation of bolus volume. The amplitude of the fit was observed to also be influenced by the time since last elution, and possibly other clinical factors. Elution times to reach the 4 activity levels were plotted vs. generator age. The linearized data was fitted and 95% confidence limits were created symmetrically around the fit. The 95% CL band allowed a prediction of elution time to achieve each bolus size for future generators, as a function only of generator age.

Conclusion: A predictive model was created for elution times from this brand of 82Rb generator as a function of generator age. The value of this model is in determining if the necessary amount of activity can be extracted from a generator before reaching one of the backup infusion settings, such as volume limits per administration, given a generator age. Some sites may also wish to control the bolus duration for better MBF calculations, since predicting the time for the injection to complete may determine if MBF and CFR calculations are meaningful.

Keywords: rubidium-82, modeling, physics

## Introduction

While both myocardial perfusion single-photon emission computed tomography (SPECT) and positron emission tomography (PET) imaging provide valuable information regarding three-dimensional distribution of radiotracers into myocardium, there are a number of physical differences where PET has a clear advantage over SPECT (*1*). PET has high spatial and temporal resolution, reliable attenuation and scatter correction, short imaging protocols utilizing short-lived positron emitting radiotracers to acquire 3-D acquisition simultaneously which offers tracer kinetic models to obtain absolute myocardial blood flow (MBF) measurements for rest and stress, where coronary flow reserve (CFR) or myocardial flow reserve (MFR) are terms interchangeable with Stress/Rest MBF, and relative perfusion and function analysis as well. These important properties of myocardial perfusion PET imaging translate into high diagnostic accuracy, consistent high-quality images, low radiation exposure, short acquisition protocols, routine quantification of MBF and strong prognostic power.

According to the American Society of Nuclear Cardiology (ASNC) and the Society of Nuclear Medicine and Molecular Imaging (SNMMI) Position Statement (*2*), rest-stress PET myocardial perfusion imaging (MPI) is a preferred test for patients with known or suspected coronary artery disease (CAD) who meet appropriate criteria and are unable to exercise adequately. Rest-stress PET MPI is recommended for patients with suspected CAD who also meet one or more of the following criteria; poor quality, equivocal or inconclusive prior stress imaging or discordant with clinical or other diagnostic test results including findings at coronary angiography; high-risk patients with advanced kidney disease, diabetic, known left main, multivessel or proximal left anterior descending artery (LAD) disease, post-heart transplant; young patients with CAD; patients who needs MBF to assess microvascular function.

According to the Joint Position Paper of SNMMI Cardiovascular Council and the ASNC (*3*), under resting condition, autoregulation of myocardial tissue perfusion occurs in response to local metabolic demands. Rest MBF has been shown to vary linearly according to the product of heart rate and systolic blood pressure (*3*, *4*). Interpretation of the stress MBF together with CFR (MFR) account for the confounding effects of resting hemodynamics (heart rate and systolic blood pressure). To ensure accurate estimates of MBF and CFR (MFR), it is critical to verify that each dynamic series is acquired and analyzed correctly. Therefore, it is important to note that consistent tracer injection profiles improve the reproducibility of MBF measurements and to ensure adequate sampling of the compete arterial blood input function (*3*).

Assessment and correction of patient motion between the first-pass transit phase and the late-phase myocardial retention images are essential, as this can otherwise introduce a large bias in the estimated MBF values compared to the relative perfusion image findings. The peak height of blood pool time–activity curves (TAC) at rest and stress should be comparable if similar radiotracer activities are injected. If there are substantial differences, extravasation or incomplete delivery of tracer may have occurred and may result in inaccurate MBF estimates. As variations in tracer injection profile could adversely affect MBF accuracy, blood pool TAC should be visually examined for multiple peaks or broad peaks, which may suggest poor-quality injections due to poor-quality IV catheters, arm positioning, or other confounding factors from patient’s physiology (*3*).

Another potential source of variability in radiotracer delivery is the 82Rb generator itself. Current recommendation is to inject a weight-based activity level to minimize population radiation dose (*5*). The ability to deliver a large dose for a large body habitus may be compromised as the generator reaches the end of its lifetime since the activity curve for the daughter isotope delivered from a generator must vary as the parent isotope decays away. The peak height of the activity curve will vary if the activity is injected as a bolus (activity concentrated in time and location) or is injected continuously as the generator struggles to produce. A recent guide from ASNC and SNMMI on PET measurements of MBF (6) recommends the following to control bolus duration for accurate MBF measurement: ensure a good free-flowing forearm intravenous line (#20 gauge or larger) for tracer administration; saline flush immediately after the tracer administration to help clear the blood pool activity; review and compare the rest and stress time-activity curves on dynamic images as a quality control; apply motion correction on dynamic images as needed; follow the weight- or BMI-based dosing consistently; schedule obese patients on earlier generator cycle to minimize administering the suboptimum tracer activity due to volume limit. The last two points regarding bolus duration and weight-based dosing are dependent on generator performance.

For these reasons, it may be of interest to develop a method for calculating the bolus length for a patient given his/her weight and the age of the generator (defined as days post-calibration). If the time to achieve complete bolus injection exceeds a level set by the nuclear cardiologist, or would exceed the infusion cart's infusion volume limit setting, then the patient will not receive the diagnostic quality as ordered. The patient may need to be rescheduled for a time when the generator is fresher, or when the next generator has been installed, or the clinical approach may need to be changed. This manuscript provides a formula for this calculation, which is based on de-identified injection printouts for an 82Rb Bracco Cardiogen generator covering its full clinical life.

## Methods

The data sample came from de-identified tickets (data output) produced by three Cardiogen (Bracco) 82Rb generators. All three were calibrated for 100 mCi (3700 MBq) and were in use for one month each, for a total of 491 elutions. Each generator was retired from clinical use after one month, following institutional policy. One generator was studied independently, and then all generator data was combined for an overall analysis. The following information was extracted from each ticket: date, time, the total injected volume, the total injected activity, and the injected activity rate at each second during the injection. For each elution, the peak injected activity rate was recorded and a calculation was made of the injection duration in seconds to inject up to four different activity levels of 20, 30, 40, and 45 mCi (740, 1110, 1480, and 1665 MBq respectively).

Two separate datasets were created for the purpose of predicting generator behavior. The first dataset was the complete injected activity curve for each injection, for the purposes of predicting the required time to administer a certain amount of activity. The injected activity rate curve of one large bolus injection was fitted using Microsoft Excel to determine the functional form of the bolus over time, and this functional form was applied to the other elutions. Once the functional form was verified, the peak injected activity rate was used as a proxy for the amplitude of the fit when comparing the individual elutions.

The second dataset consisted of the time to reach four different injected activity level as a function of the age of the generator, in days since calibration. 95% confidence bands were created for each of the chosen activity levels by fitting the data in OriginPro (OriginLab Corporation) using an exponential growth function of the form $y(t) = y_0 + A \cdot EXP\left(\frac{t}{t1}\right)$. A band was created symmetrically around the fit by shifting $y_0$ (the y intercept) by ±Δy to encompass 95% of the data between the shifted curves. The fit and 95% CL band allowed a prediction of time to achieve that bolus size for future generators as a function of generator age.

## Results

The plot of injected activity per second over time for a single large bolus was well fitted by a growth-saturation model of the form $y(t) = y_0 + A \cdot (t - t_0) \cdot EXP\big(-C \cdot (t - t_0)\big)$, shown in Figure 1. The reduced chi-squared of the fit was 0.61 using an uncertainty of 5% on the activity from the injection cart's dose calibrator. This model allowed the calculation of the total injected activity at any time during the elution. However, the peak injected activity rate did not follow an exponential decay with the age of the generator but peaked within a week of the calibration date of the generator. Also, the peak injected activity rate fluctuated throughout the day, as shown by the spread of peak injection activity rates in Figure 2.

The time to administer four different injected activity levels separated into distinct regions, although the bands that contained 95% of the data did overlap at low generator ages, as shown in Figure 3. The 20 mCi (740 MBq) activity level band contained results from 459 elutions, the 30 mCi (1110 MBq) band contained results from 454 elutions, the 40 mCi (1480 MBq) band contained results from 169 elutions, and the 45 mCi (1665 MBq) band contained results from 60 elutions. The parameters of the best fit to the data, along with the Δy of the 95% bands, are listed in Table 1. These are the parameters of four exponential growth models (for the four target activity levels studied) of the form $y(t) = y_0 + A \cdot EXP(t/t_1)$, where $y(t)$ is the time to achieve a certain bolus of activity given a generator age $t$, $y_0$ is the threshold time (the generator is being eluted but activity is not injected until a threshold of 1.0 mCi (37 MBq) per second), $A$ is the amplitude (s) and $t_1$ is the growth constant. Given the age of the generator, the user can calculate the duration of the bolus in seconds that will produce one of the four activity levels described. Alternatively, the user can take an upper limit for the bolus duration and use the formula $t = t_1 \cdot \ln\left(\frac{y-y_0}{A}\right)$ to calculate the last day of generator life where that bolus can (on average) be achieved.

Some data was excluded from this fit; data from the first three days of each generator, when the peak activity rate was increasing, was removed. Also, a single generator had data from two days that did not conform to the distribution of the other points, as evidenced by a large residual to the fit, and was removed.

**Discussion**

Although the injected activity rate was well-fitted, the amplitude did not depend solely on the physics of radioactive decay. It was observed that the peak output activity rate (used as a proxy for the amplitude in the growth-saturation fit) increased for the first few days of use then decreased throughout the week, except the rate did not decrease consistently over the weekend. Note that the generator was not used over the weekend, but the data in Figure 2 for Fridays and Mondays does not show a consistent pattern. Following a similar pattern, a correlation between peak injection activity rate and length of time since last elution was observed.

82Sr and 82Rb are in secular equilibrium and a generator that is eluted every 10 minutes will have a daughter/parent ratio of 99.7%; clinical practice dictates no less than 10 minutes between elutions, so a correlation was unexpected. The correlation was determined using Pearson's method to produce a coefficient and correlation likelihood; for one generator, 100% of days with clinical usage showed a 95% likelihood or greater correlation between eluted peak activity rate and generator rest times. This positive correlation held true even out to 350 minutes since last elution, which is more than 2 orders of magnitude greater than the half-life of the 82Rb daughter isotope. The variation in peak output due to time since last elution (a maximum difference of 10%) is greater than the variation between days as the generator ages, as shown in Figure 4. Although longer rest times will have some marginal benefit to bolus lengths as the generator ages, the variability of peak output with generator rest times is one of the confounding factors in presenting a completely deterministic model.

These two complications are consistent with findings from the initial development of the 82Sr/82Rb generator by TRIUMF (*7*). As the generator was eluted over time, the distribution of 82Sr within the generator column changed from a narrow band at the top of the column to a much broader peak towards the bottom. Therefore, one would expect the diffusion rate to be higher later in the generator's life because of the greater surface area covered with 82Sr. In private communication with a Bracco scientist, it was confirmed that rest periods longer than ten minutes should result in greater activity in solution as chemical equilibrium has not yet been reached.

Regarding the fit to the second dataset, it was noted that the prediction band for the 45 mCi (1665 MBq) had much less precision than the bands for other activity levels, having a band width of 8 sec compared to 1-2 sec for 20 and 30 mCi (740 and 1110 MBq) activity levels. Subtracting one day of data from each of two different generators reduced the band width to 2.5 sec while keeping 52 of the 60 data points. Although there is no *a priori* justification for this change to the dataset, it does suggest that the true distribution of bolus times is more narrow and that there is an uncontrolled variable causing longer elution times on certain days. One possibility is that the IV gauge used clinically was different for those two days, since the elution times were significantly longer given the eluted activity.

The clinical significance of the model was varied across different dose limits. The effect of the bolus lengthening can be best seen at 42 days, which is the generator expiry limit. For an elution of 20 mCi (740 MBq), the model predicts an elution time of 13 seconds at day 42, which is not much more than the 8.5 seconds predicted for day 2. Meanwhile, the 45 mCi (1665 MBq) model predicts an elution time of 110 seconds at day 42, in contrast to the 17 seconds required on day 2.

Our institution limits the infusion to 50 mL to patient, which although more restrictive than the prescribing information limit of 100 mL, may be more relevant to clinical practice. With a flow rate setting of 50 mL/min, and a startup time of approximate 14 seconds, the maximum elution time is 74 seconds before triggering the elution to stop. For a cutoff time of 74 seconds, the model predicts that the last day to achieve 45 mCi (1665 MBq) is day 34; the last day to achieve 40 mCi (1480 MBq) is day 42. The other two activity levels, 20 and 30 mCi (740 and 1110 MBq), will not be limited before the expiry of the generator.

## Conclusion

In conclusion, we were able to develop predictions for the time to elute a bolus of certain durations from a 82Rb generator as a function of generator age. Given the flow rate (mL/min) setting selected by the user, the volume of the bolus can be determined from the duration of the elution. Although the eluted activity rate over time was well fitted by a growth-saturation curve, the amplitude of this curve was not just dependent on generator age but also factors such as generator rest times and likely clinical factors such as patient circulatory resistance and IV gauge as well.

There were real instances of truncated elutions; within the datasets collected there were a few elutions where full prescribed activity was not delivered due to triggering the limit on patient volume (50 mL). For a 45 mCi (1665 MBq) prescribed activity on day 31 of the generator, the elution was cutoff at 72 seconds due to hitting the patient volume limit, and this is within the prediction range. The prediction bands for different activity levels allow for a range of bolus injection times that run up to 66 ± 8 sec for 45 mCi (1665 MBq) on day 31.

The consequences of performing a coronary flow reserve exam using a bolus duration of 61 sec (45 mCi, or 1665 MBq, on day 30) could include erroneous MFR calculations. The authors did check our records for patients with MFR calculations and whose exams resulted from different 82Rb generators, but the data was sparse as this information was included somewhat recently. We plan to test our predictions on future generators to determine the broader applicability and to evaluate the clinical impact once more multi-year records are available.

## Acknowledgments

The authors wish to acknowledge Jeffrey Metcalf, CNMT for his assistance in collecting the data, Dr. Adrian Nunn of Bracco Imaging for information on Rb-82 generators, and Dr. Dan Berman, FACC for contributing to the original research concept.

**Key Points**

Question: Can a Rb-82 generator bolus duration be predicted as a function of activity eluted and the generator age?

Pertinent findings: For a particular generator model, the activity output rate was fitted with a growth-saturation curve and the times to achieve certain eluted activities were fitted as a function of generator age using an exponential curve and symmetric bands to capture 95% of the data points.

Implications for patient care: Utilizing these calculations allows patients to be rescheduled if their predicted injection time given the prescribed Rb-82 activity and generator age would exceed the preset bolus duration limit.

**References**


1. Dilsizian, V. Transition from SPECT to PET myocardial perfusion imaging: A desirable change in nuclear cardiology to approach perfection. *J Nucl Cardiol*. 2016 Jun; 23 (3):337-8.
2. Bateman T, Dilsizian V, Beanlands R, DePuey, E, Heller G, Wolinsky D. American Society of Nuclear Cardiology and Society of Nuclear Medicine and Molecular Imaging Joint Position Statement on the Clinical Indications for Myocardial Perfusion PET. *Journal of Nuclear Medicine.* 2016 Oct; 57 (10) 1654-6.
3. Murthy VL, Bateman TM, Beanlands RS, Berman DS, Borges-Neto S, Chareonthaitawee P, *et al.* Clinical Quantification of Myocardial Blood Flow Using PET: Joint Position Paper of the SNMMI Cardiovascular Council and the ASNC. *Journal of Nuclear Medicine.* 2018 Feb; 59(2): 273-93.
4. Nagamachi S, Czernin J, Kim AS, Sun KT, Bottcher M, Phelps M, *et al*. Reproducibility of measurements of regional resting and hyperemic myocardial blood flow assessed with PET. *Journal of Nuclear Medicine*. 1996;37:1626–31.
5. Case JA, deKemp RA, Slomka PJ, Smith MF, Heller GV, Cerqueira MD. Status of cardiovascular PET radiation exposure and strategies for reduction : An Information Statement from the Cardiovascular PET Task Force. *J Nucl Cardiol*. 2017 Aug: 24(4): 1427-39.
6. Bateman TM, Heller GV, Beanlands R, Calnon DA, Case J, deKemp R, *et al*. Practical guide for interpreting and reporting cardiac PET measurements of myocardial blood flow: An information statement from the American Society of

Nuclear Cardiology and the Society of Nuclear Medicine and Molecular Imaging. *Journal of Nuclear Medicine.* 2021 March.

7. Crackette, Ruth V. 82-Sr Production from metallic Rb targets and development of an 82-Rb generator. *Appl Radiat Isot*. 1993;44(6):917-922.

**Tables**

| | y-intercept (y0), seconds | Amplitude (A), seconds | Growth constant (t1), days$^{-1}$ | Band range (seconds) |
|---|---|---|---|---|
| 20 mCi fit | 6.05 | 2.31 | 37.54 | ±1.05 |
| 30 mCi fit | 6.25 | 5.21 | 32.60 | ±1.70 |
| 40 mCi fit | 9.25 | 5.70 | 17.33 | ±5 |
| 45 mCi fit | 2.93 | 13.12 | 20 | ±8 |
| Modified 45 mCi fit | 16.22 | 3.15 | 10.96 | ±2.5 |

*Table 1 Fit parameters for time to elute certain activity levels as a function of generator age, following the functional form* $y(t) = y_0 + A \cdot EXP\left(\frac{t}{t1}\right)$. *An additional fit was performed for the largest eluted activity (1665 MBq) to demonstrate that the data could be more precisely fitted absent two days' worth of generator results.*

## Figures

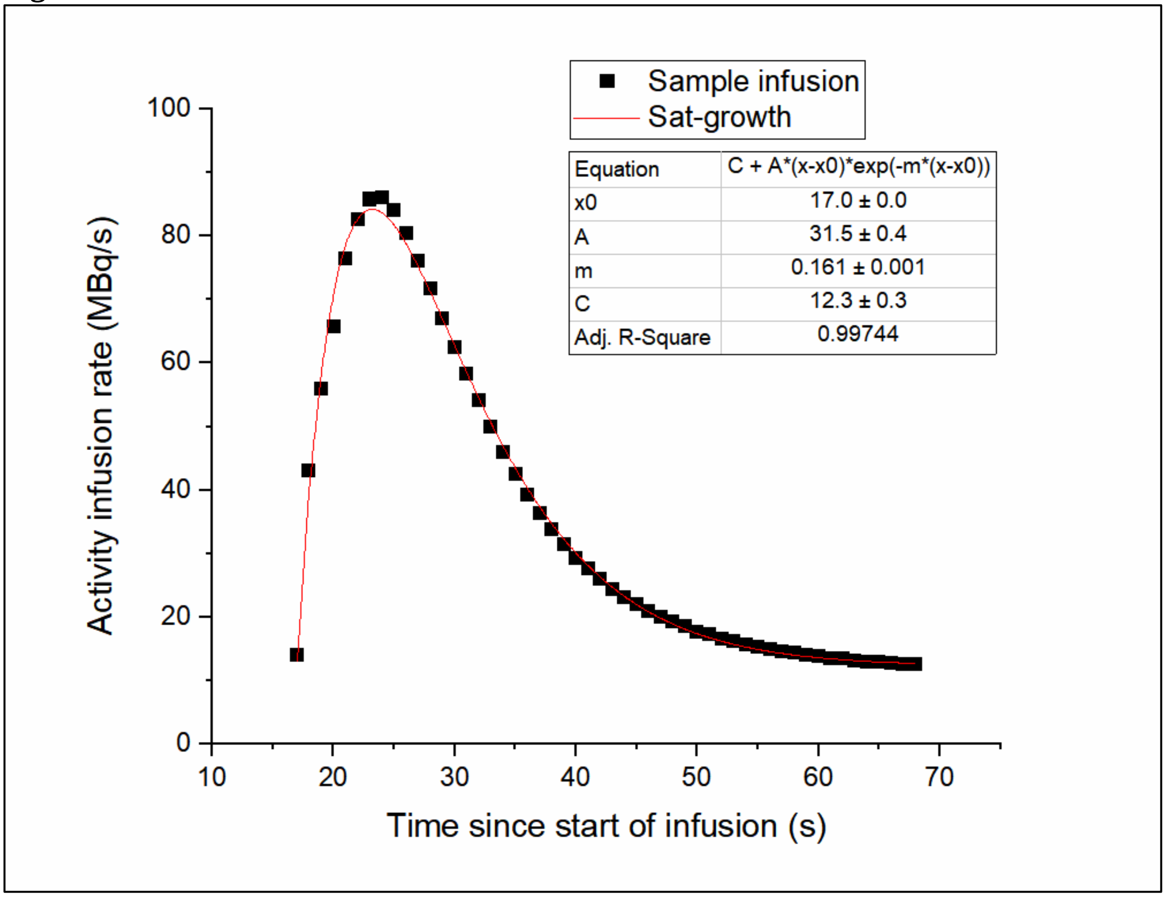


*Figure 1 (left) Activity infusion rate data and fit for sample bolus from 2/9/2017, with fit parameters for a growth-saturation curve of the form* $y(t) = C + A \cdot (t - t_0) \cdot EXP(-m \cdot (t - t_0))$.

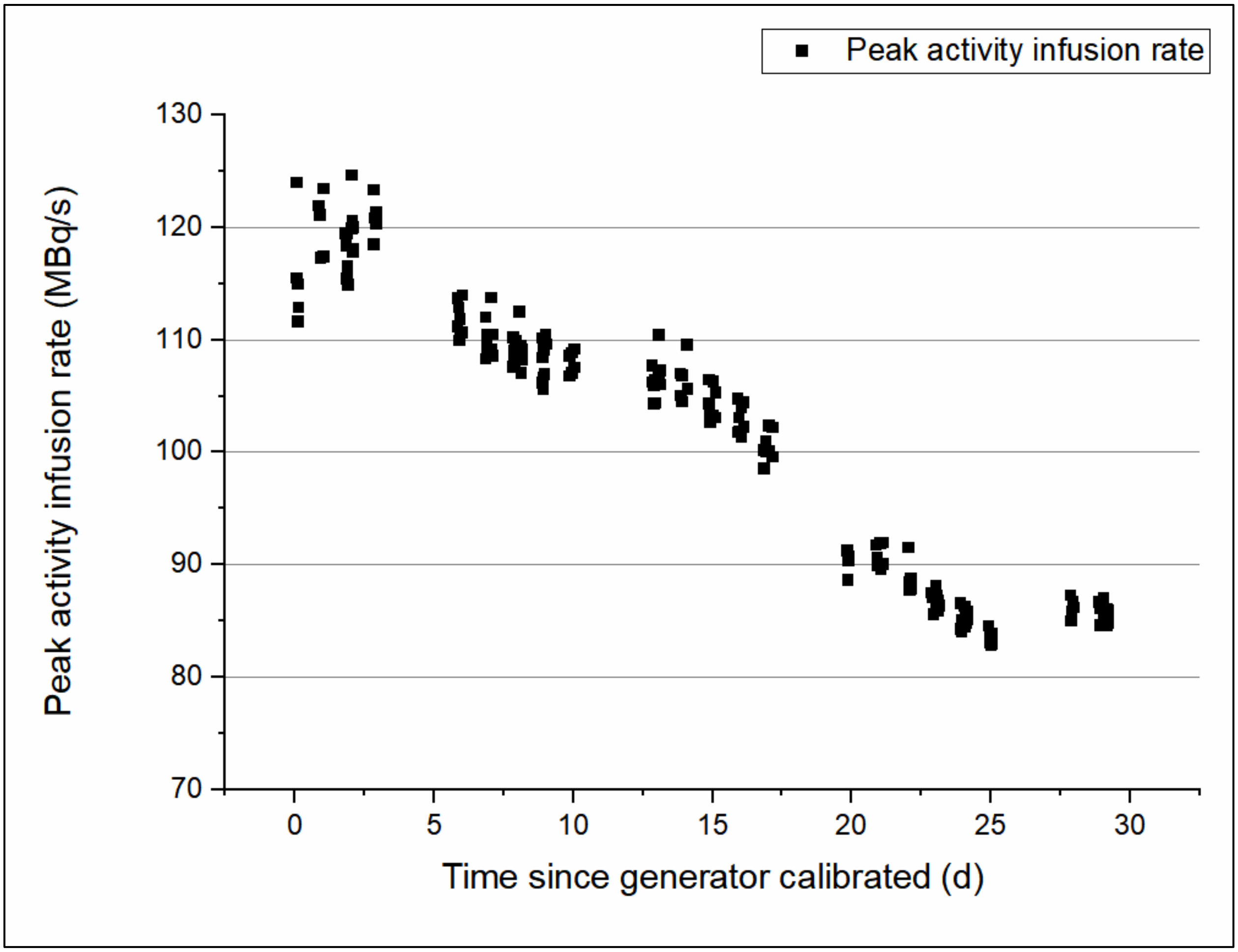


*Figure 2 (Right) Peak activity infusion rate for each study from one representative generator as a function of generator age. The amplitude of the activity rate curve did not decrease exponentially with generator age as expected. There is also up to 10% variation in peak activity rates within a single day.*

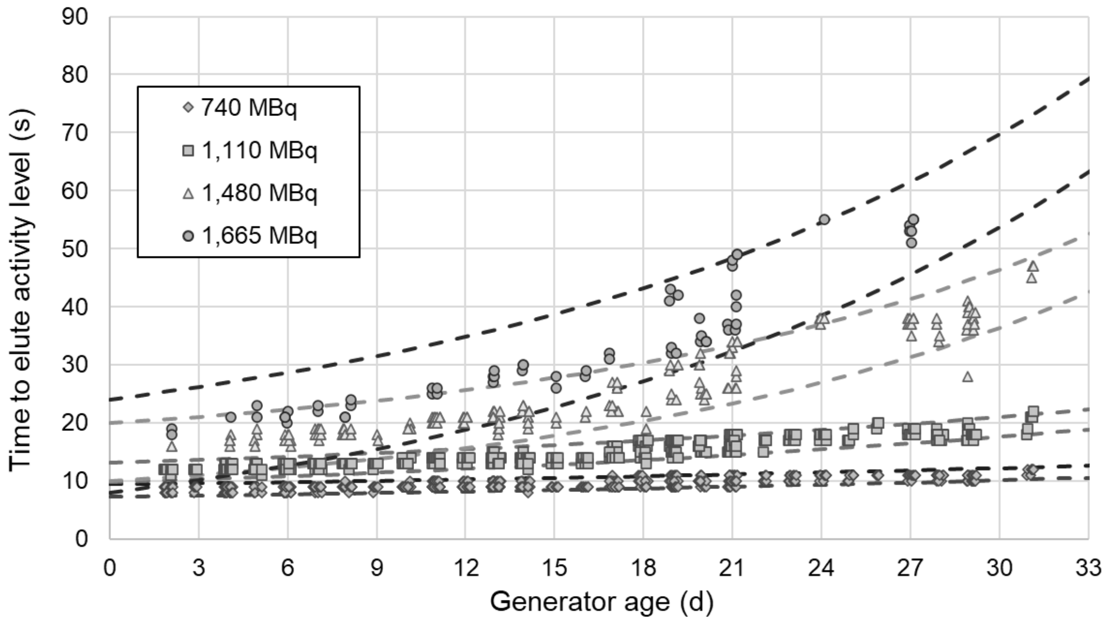


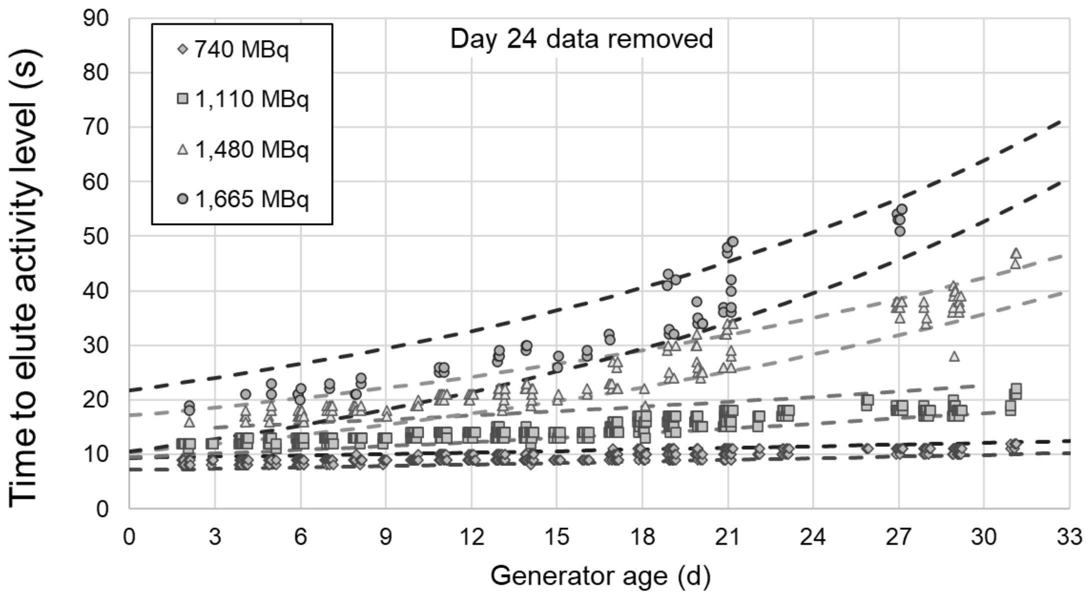


*Figure 3: Best fit bands for four activity levels and time to elute each, as a function of generator age. Each band contains 95% of the data points for each injected activity level. The data is combined from three separate 82Rb generators. Top image is with anomalous results from day 24, bottom image is without.*

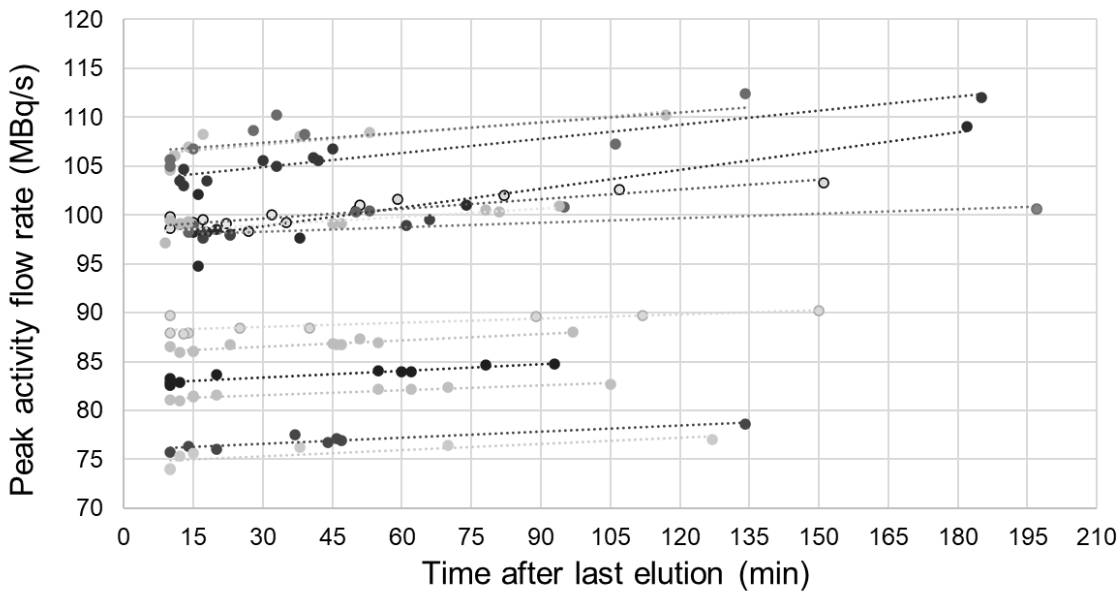


*Figure 4: peak activity injection rate for each elution, compared to time since last elution. Lines connect data from the same day, such that the points come from the same generator age. Ten minutes is the minimum spacing for clinical usage and no studies had a time-since-last-elution less than this value. Based on secular equilibrium assumptions, the 82Rb / 82Sr ratio should be 99.7% of its maximum at 10 minutes. The elution continues to produce higher peak activity rates with resting times up to 3 hours, the longest time measured.*

Graphical Abstract